View metadata, citation and similar papers at core.ac.uk

brought to you by CORE

provided by Elsevier - Publisher Connector

Available online at www.sciencedirect.com

ScienceDirect

Energy Procedia 52 (2014) 536 – 540

Energy Procedia

2013 International Conference on Alternative Energy in Developing Countries and Emerging Economies

Voltage and frequency dependent impedances of dye-sensitized solar cell

Thossaporn Pongklang[a], Dhirayut Chenvidhya[b,*], Krissanapong Kirtikara[b], Surawut Chuangchote[c], Nitikorn Silsirivanich[b]

[a]*Division of Energy Technology, School of Energy, Environment and Materials,*
[b]*CES Solar Cells Testing Center, Pilot Plant Development and Training Institute,*
[c]*The Joint Graduate School of Energy and Environment*
King Mongkut's University of Technology Thonburi,
126 Pracha-uthit Rd., Bangmod, Thungkru, Bangkok 10140, Thailand.

Abstract

This paper describes a derivation of the dynamic impedance of a dye-sensitized solar cell (DSSC) and its characterization using a frequency response analyzer (FRA). The dynamic impedance equation as a function of voltage and frequency is presented. Testing is done on a DSSC, fabricated from a fluorine-doped SnO_2 (FTO) conducting glass, ruthenium (II) dye (N719) sensitized TiO_2 nanoparticles, an iodide-triiodide electrolyte, and a Pt counter electrode. At each bias voltage, impedance locus is plotted in a complex plane. Intercepts of each semicircular impedance loci yield series, dynamic, and shunt resistance of the cell. Experimental results could be used to analyze characteristics of AC equivalent circuit components.

© 2014 Published by Elsevier Ltd. This is an open access article under the CC BY-NC-ND license (http://creativecommons.org/licenses/by-nc-nd/3.0/).
Selection and peer-review under responsibility of the Organizing Committee of 2013 AEDCEE

Keywords: Dye-sensitized solar cell, dynamic impedance model, frequency response, equivalent circuit ;

1. Introduction

Dye-sensitized solar cells (DSSCs) have received much interest as possible future low cost solar cells as DSSCs use inexpensive materials and simple processes. To improve cell performance for wide-scale applications, understanding of parameter behaviors through equivalent circuit modeling are important,

* Corresponding author. Tel.: +662-470-8626; fax: +662-427-8077.
E-mail address: dhirayut.che@kmutt.ac.th.

1876-6102 © 2014 Published by Elsevier Ltd. This is an open access article under the CC BY-NC-ND license (http://creativecommons.org/licenses/by-nc-nd/3.0/).
Selection and peer-review under responsibility of the Organizing Committee of 2013 AEDCEE
doi:10.1016/j.egypro.2014.07.107

especially dynamic behavior. DSSC dynamic parameters can be determined by using impedance spectroscopy through a variety of characterization methods. In previous works [1-4], impedance characteristics of c-Si and a-Si solar cells have been presented and analyzed. In this paper, we derive the dynamic impedance of a DSSC under dark using a FRA. Voltage and frequency dependences of DSSC dynamic parameters are shown.

In general, a DSSC is composed of a transparent conducting oxide (TCO) glass covered with metal oxide (i.e.TiO_2), dye molecules attached to the surface of metal oxide, a redox couple electrolyte, and a catalyst (i.e., platinum) coated on transparent conducting glass as a counter electrode. Under illumination the AC or dynamic equivalent circuit of a DSSC when connecting to a load can be represented as Fig. 1(a) [5-6]. Resistance 1 (R_1) and capacitance 1 (C_1) are elements of impedance 1 (Z_1) due to redox reaction at the platinum counter electrode. Z_2 represents as a diode, taking into account electron transfer at the TiO_2/dye/electrolyte interfaces. R_3 and C_3 are elements of Z_3 relating to carrier transport of ions within the electrolyte. Shunt resistance (R_{sh}) accounts for back electron transfer across the TiO_2/dye/electrolyte junctions. Sheet resistance (R_s) accounts for the transport resistance of TCO substrate.

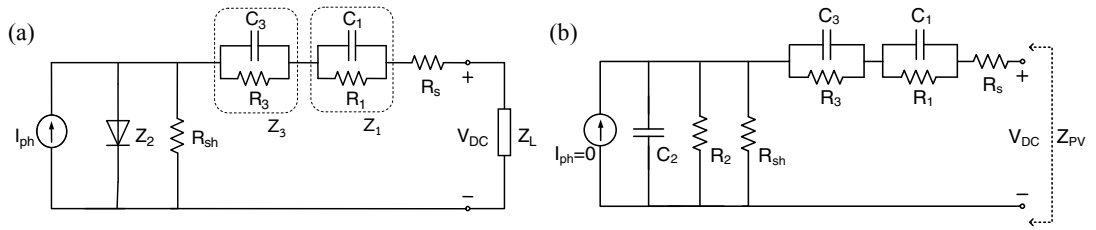

Fig. 1. AC equivalent circuit model of a DSSC; (a) connecting to a load (Z_L) under illumination, and (b) when consider Z_2 as two parameters under dark condition.

2. Experiment

The DSSC under test is fabricated from a fluorine-doped SnO_2 (FTO) conducting glass, ruthenium (II) dye (N719) sensitized TiO_2 nanoparticles, an iodide-triiodide electrolyte, and a Pt counter electrode. It has an area of 0.6 cm^2. Under 1 sun, air mass 1.5 illumination and standard test conditions, the DSSC shows a short circuit current density (J_{SC}) of 0.72 mA/cm^2 and an open circuit voltage (V_{OC}) of 0.49 V.

The DSSC is investigated under dark conditions, at room temperature, using a FRA (impedance gain - phase analyzer, Solartron 1260) under both forward and reverse biases of 0.2, 0.3, and 0.4 V. The amplitude of a small AC signal superimposing on the DC bias is about 10% of the bias level. The AC signal is in the frequency range of 0.01 Hz to 200 kHz. Frequency response measurement results are plotted as impedance loci in the complex plan, and separate magnitude and argument plots.

3. Results and Discussion

In this study, we consider Z_2 (Fig. 1(a)) as two parameters in parallel (Fig. 1(b)), *i.e.* diode resistance (R_2) and diode capacitance (C_2). Under dark condition, looking at an output port, we can model the photovoltaic impedance (Z_{PV}) as consisting of a resistive and a reactive component in series in the form of $R_{PV} + jX_{PV}$. At each bias voltage (V) and signal frequency (ω), the impedance can be expressed as equation (1).

$$Z_{pv}(V,\omega) = R_{PV}(V,\omega) + jX_{PV}(V,\omega)$$
$$= R_S + \left[\frac{R_1}{(\omega C_1 R_1)^2 + 1} + \frac{\left[\{R_{sh} + R_2(V)\}R_{sh}R_2(V)\right]}{\left[\omega R_{sh}R_2(V)\{C_2(V,\omega)\}\right]^2 + \left[R_{sh} + R_2(V)\right]^2} + \frac{R_3}{(\omega C_3 R_3)^2 + 1}\right]$$
$$- j\left[\frac{\omega C_1 R_1^{\,2}}{(\omega C_1 R_1)^2 + 1} + \frac{\omega\{R_{sh}R_2(V)\}^2\{C_2(V,\omega)\}}{\left[\omega R_{sh}R_2(V)\{C_2(V,\omega)\}\right]^2 + \left[R_{sh} + R_2(V)\right]^2} + \frac{\omega C_3 R_3^{\,2}}{(\omega C_3 R_3)^2 + 1}\right] \quad (1)$$

$$Z_{pv} = R_{PV} + jX_{PV}$$
$$= R_S + \left[\frac{R_1}{(\omega C_1 R_1)^2 + 1} + \frac{R_p}{(\omega C_2 R_p)^2 + 1} + \frac{R_3}{(\omega C_3 R_3)^2 + 1}\right]$$
$$- j\left[\frac{\omega C_1 R_1^{\,2}}{(\omega C_1 R_1)^2 + 1} + \frac{\omega C_2 R_p^2}{(\omega C_2 R_p)^2 + 1} + \frac{\omega C_3 R_3^{\,2}}{(\omega C_3 R_3)^2 + 1}\right] \quad (2)$$

For simplification, we drop V and ω, and lump R_{sh} and R_2 ($R_{sh}//R_2$) into parallel resistance (R_P). The simplified dynamic impedance equation can be rewritten as equation (2).

It should be noted that C_2 are voltage and frequency dependent, and R_2 is voltage dependent [1-2].

Dynamic impedances under both forward and reverse biases at 0.2, 0.3, and 0.4 V are determined by FRA under dark conditions. Impedance loci are plotted in a complex plane as shown in Fig. 2. It is found that, the impedance loci are semicircles and conform to equation (2). At high and low frequencies for

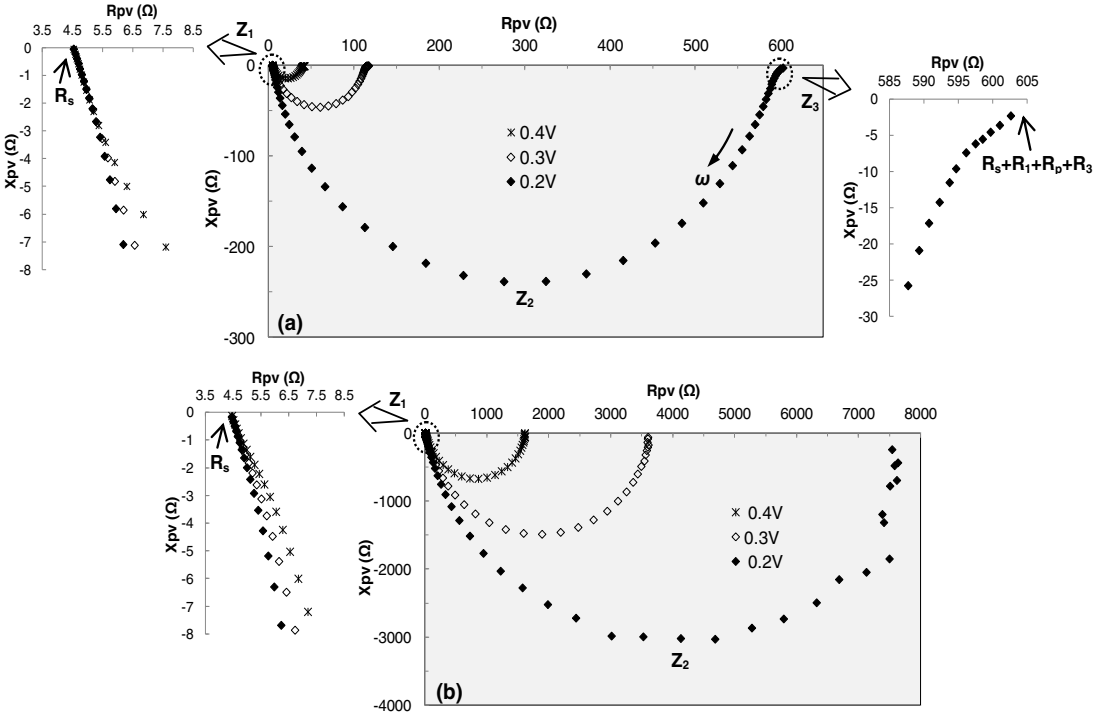

Fig. 2. Impedance loci of the DSSC; (a) under forward biases, and (b) under reverse biases.

each bias voltage, reactive component (X_{PV}) approaches to zero. Resistive component (R_{PV}) is approximately equal to R_S at high frequencies (mega Hz region), while it is equal to $R_S+R_1+R_P+R_3$ at low frequencies (milli Hz region). In general, at each bias voltage, 3 semicircles should be obtained from impedance locus. However, results of our test cell show that R_1 and R_3 are relatively low. So only one semicircle, Fig. 2(a), is observed. On the other hand, if we examine closely, using expanded scales, we can distinguish other resistances. The diameter of each semicircle is equal to R_1, R_P and R_3, as the resistive component of Z_1, Z_2, and Z_3, respectively. The DSSC resistances from experimental results at any bias voltage are shown in Table 1.

Table 1. The DSSC resistances under both forward and reverse bias at 0.2, 0.3, and 0.4 V

Biasing voltage (V)	R_S (Ω)	R_1 (Ω)	R_p (Ω)	R_3 (Ω)
Forward bias				
0.2	4.53	1.02	591.36	7.09
0.3	4.53	1.02	109.25	6.78
0.4	4.53	1.01	35.49	7.02
Reverse bias				
0.2	4.52	1.01	7533.08	0
0.3	4.52	1.02	3594.48	0
0.4	4.52	1.03	1607.18	0

In Table 1, at each bias voltage, the sum of R_S, R_1, and R_3 is equal to series resistance of a cell. Under different applied voltage levels, one sees an apparent change in only R_P, and is similar to that reported by Han et al. [6].

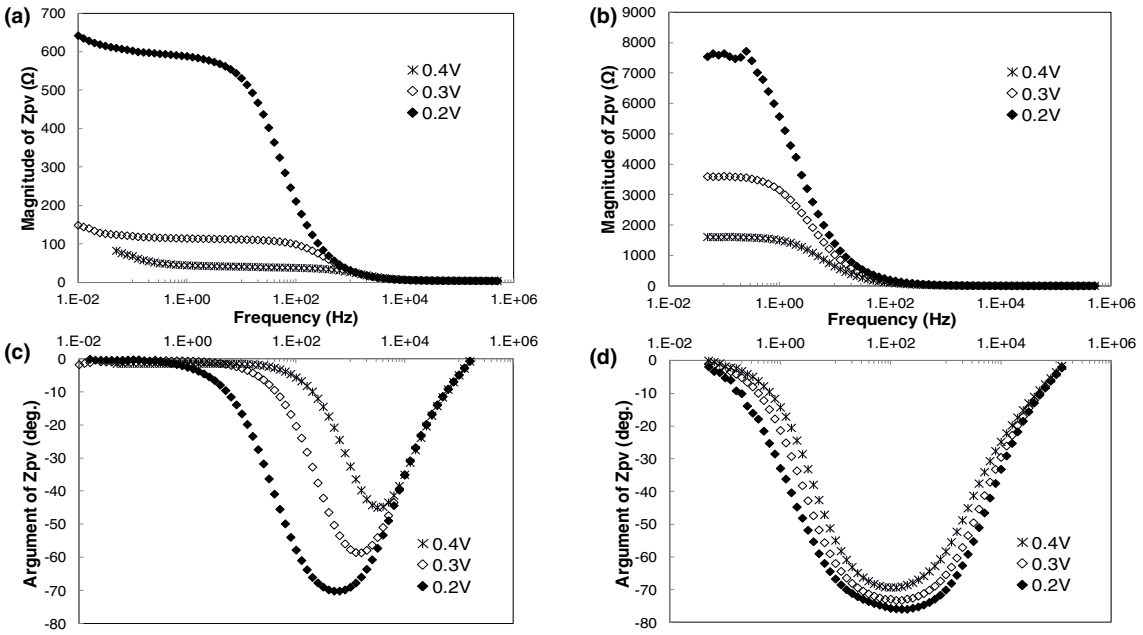

Fig. 3. Magnitude and argument of impedance plots as function of frequency; (a) magnitude plot under forward biases, (b) magnitude plot under reverse biases, (c) argument plot under forward biases, and (d) argument plot under reverse biases.

For this study, R_P is equal to ($R_{sh}R_2/(R_{sh}+R_2)$). Under forward bias, assuming that R_{sh} is much greater than R_2 (R_{sh}»R_2), so R_P is approximately equal to R_2. In Fig. 2, we note that R_2 is voltage dependent, and decreases with increasing voltage. It is clearly observed that R_2 in the equivalent circuit of a DSSC exhibits similar behaviour with dynamic resistance R_d of p-n junction solar cells [3-4].

Under low reverse biases, R_2 is very large compared with R_{sh} (R_2»R_{sh}), so R_P is approximately equal to R_{sh}. For our cell, R_{sh} is 7.5 kΩ , approximated at a reverse bias voltage of 0.2 V.

From impedance loci, we can plot magnitude and argument of impedance as shown in Fig.3. We clearly see the voltage and frequency dependent nature of the impedance.

4. Conclusion

In this paper, dynamic impedance of a DSSC is derived from the AC equivalent circuit and experimental results. Impedance measurements are done by using a FRA under dark condition. The nature of voltage and frequency dependent impedance of the DSSC is also illustrated. The dynamic impedance of the DSSC can yield information and explain the parameter behaviors. The simple method described in this paper can be used to investigate series, dynamic, and shunt resistance of DSSC. Moreover, the dynamic impedances developed in this work can be further applied for the comparison of the DSSC performance.

Acknowledgements

The authors wish to acknowledgment supports from the CES Solar Cells Testing Center (CSSC) for excellent research facilities.

References

[1] Chenvidhya D, Kirtikara K, Jivacate C. On dynamic and static I-V characteristics of solar cells modules having low and high fill factors. *Proceedings of 3rd World Conference on Photovoltaic Energy Conversion (WCPEC-3)*, Osaka: Institute of Electrical and Electronics Engineers; May 2003, p.1927-1929.

[2] Chenvidhya D, Kirtikara K, Jivacate C. PV module dynamic impedance and its voltage and frequency dependencies. *Sol. Energy Mater. Sol. Cells* 2005; **86**: 243-51.

[3] Chenvidhya D, Kirtikara K, Jivacate C. A new characterization method for solar cell dynamic impedance. *Sol. Energy Mater. Sol. Cells* 2003; **80**: 459-64.

[4] Chenvidhya D, Limsakul C, Thongpron J, Kirtikara K, Jivacate C. Determination of solar cell dynamic parameters from time domain responses. *The 14th Photovoltaic Science and Engineering Conference (PVSEC-14)*, Thailand: Energy Conservation Promotion Fund of Thailand; January 2004.

[5] Koide N, Islam A, Chiba Y, Han L. Improvement of efficiency of dye-sensitized solar cells based on analysis of equivalent circuit. *J. Photochem. Photobiol. A-Chem.* 2006; **182**: 296-305.

[6] Han L, Koide N, Chiba Y, Islam A, Mitate T. Modeling of an equivalent circuit for dye-sensitized solar cells: improvement of efficiency of dye-sensitized solar cells by reducing internal resistance. C. R. Chim. 2006; **9**: 645-51.